ELSEVIER

Journal of Organometallic Chemistry 570 (1998) 155–162

Journal of Organometallic Chemistry

Syntheses, electrochemistry and crystal structure studies of novel *cis*-configuration biferrocene trinuclear complexes

Chun-Ying Duan [a,*], Yu-Peng Tian [a], Ze-Hua Liu [a], Xiao-Zeng You [a], Thomas C.W. Mak [b]

[a] *Coordination Chemistry Institute, State Key Laboratory of Coordination Chemistry, Nanjing University, Nanjing, 210093, China*
[b] *Chemistry Department of the Chinese University of Hong Kong, Hong Kong*

Received 18 November 1997; received in revised form 1 April 1998

Abstract

The syntheses and characterization of novel biferrocene trinuclear complexes for Schiff base ligand, *S*-methyl-*N*-(ferrocenyl-1-methyl-methylidene)dithiocarbazate (hereafter abbreviate as HL), are described. X-ray diffraction studies established the structures of the palladium complex, PdL_2 **2** and the copper complex, CuL_2 **3**. The geometry of Pd(II) in **2** is close to square planar and in novel *cis*-configuration with two ferrocene moieties in the same side, while that of Cu(II) in **3** is close to tetrahedral configuration. Electrochemical measurements suggest that the distorted square planar configuration of the Ni(II) and Pd(II) moieties, can effectively transmit the redox effects of the ferrocene moieties, while the distorted tetrahedral configuration of Cu(II) complex can not transmit the redox effects.

Keywords: Biferrocene; *Cis*-configuration; Electrochemistry; Crystal structure

1. Introduction

Bridged biferrocenes have been proven to be good candidates for mixed-valence compounds owing to their variability in structure and suitability for study with several physical techniques such as ^{57}Fe Mössbauer spectra, EPR, near-IR and IR spectra [1,2]. It has been postulated that the intervalence transfer may be accomplished in two different ways, through ligand and through space [3]. The first takes place through a bridge or a single bond between the ligands of two ferrocene units. The second occurs via direct metal–metal interaction. It is often difficult to determine which mechanism is dominant in a particular case. By the proper choice of model system, one should be able to distinguish qualitatively as to which is a more important mechanism for electron transfer in the ferrocene–ferricenium system.

It is the purpose of this paper to report the design, synthesis and structural characterization of metal bridged biferrocene trinuclear complexes derived from the Schiff-base ligand, HL, *S*-methyl-*N*-(ferrocenyl-1-methyl-methylidene)-dithiocarbazate, the relative long iron–iron distances could minimize the through space interaction, the extensive electron delocalization of the whole molecule might maximize the through ligand interaction, and the variety coordination configuration of different bridging metal moieties can also help us to determine the possible mechanism of the electron transfer.

2. Experimental detail

2.1. General comments

All chemicals are of reagent grade and used without further purification. *S*-methyl-dithiocarbazate was synthesized according to the literature method [4]. Elec-

* Corresponding author. Fax: +86 25 3317761.

0022-328X/98/$ - see front matter
PII S0022-328X(98)00583-X

tronic absorption spectra were obtained on a Shimadzu 3100 spectrophotometer in dichloromethane solution. Solid state electronic spectra were obtained by reflectance technique on a Shimadzu UV-240 spectrophotometer using MgO as reference material. IR spectra were recorded on a Nicolet FT-IR-170SX instrument (KBr discs) in the 4000–400 cm^{-1} region, The far-IR spectra (500–100 cm^{-1}) were recorded in Nujol mulls between polyethylene sheets. Elemental analyses of carbon, nitrogen, and hydrogen were performed on a Perkin-Elmer 240 analytical instrument.

2.2. Synthesis of the free ligand $[Cp_2Fe]C(CH_3)NNHCSSCH_3$ **HL**

Five drops of acetic acid were added to a mixture of *S*-methyl-dithiocarbazate (1.22 g, 10 mmol) and acetylferrocene (2.28 g, 10 mmol) in refluxing ethanol (50 ml). The solution was further refluxed for 2 h and on cooling a red–brown solid was formed. The solid was collected by filtration and washed with ethanol and dried under vacuum. Yield 0.28 g (85%) for the free ligand. Anal. Found: C, 50.8; H, 4.8; N, 7.9. $C_{14}H_{16}N_2S_2Fe$ Calc.: C, 50.6; H, 4.8; N, 8.4%.

2.3. Synthesis of the metal complexes

2.3.1. NiL_2 **1**

Ethanol solutions (25 ml) of the ligand (0.66 g, 2 mmol) and $Ni(CH_3COO)_2 \cdot 4H_2O$ (0.24 g, 1 mmol) were mixed. The brown crystalline solid formed after refluxing for 4 h was collected by filtration, washed with ethanol (3 × 10 ml) and dried under vacuum. Yield 0.50 g (69%) of the nickel complex. Anal. Found: C, 46.7; H, 4.5; N, 7.5. $C_{28}H_{30}N_4S_4Fe_2Ni$ Calc.: C, 46.6; H, 4.2; N, 7.8%.

Table 1
Crystallographic data

Compound	PdL_2 2	CuL_2 3
Formula	$C_{28}H_{30}N_4S_4Fe_2Pd$	$C_{28}H_{30}N_4S_4Fe_2Cu$
Formula weight	768.9	726.0
Colour/habit	Red-brown prism	Black plate
Size (mm)	0.30 × 0.40 × 0.50	0.40 × 0.15 × 0.50
Crystal system	Monoclinic	Orthorhombic
Space group	C_2/c	Pbca
Unit cell dimensions		
a (Å)	18.859 (1)	15.415 (1)
b (Å)	14.400 (1)	19.477 (1)
c (Å)	11.203 (1)	19.938 (1)
β (°)	105.97 (1)	
V (Å^3)	2925 (2)	5986 (3)
Z	4	8
μ (cm^{-1})	19.0	19.6
d_{calcd} (g cm^{-3})	1.75	1.61
F(000)	1552	2968
Temperature (K)	294	294
λ (Å)	0.71073	0.71073
Reflections collected	5222	20 733
Reflections unique	2898 (R_{int} = 2.02%)	6311 (R_{int} = 7.3%)
Reflections observed	2862 ($F_o > 4.0\sigma(F)$)	5564 ($F_o > 4.0\sigma(F)$)
R	0.039	0.061
Rw	0.051 ($w^{-1} = \sigma^2(F)$)	0.077 ($w^{-1} = \sigma^2(F)$)
$(\Delta\rho)_{max,min}$ eÅ^{-3}	0.58, −1.18	1.30, −0.83

Table 2
Atomic coordinates(10^4) and equivalent isotropic displacement coefficients (Å × 10^3) for palladium complex **2**

Atom	*x*	*y*	*z*	U_{eq}
Pd (1)	0	787 (1)	2500	36 (1)
Fe (1)	−1212 (1)	3355 (1)	−502 (1)	33 (1)
S (1)	528 (1)	−331 (1)	1621 (1)	53 (1)
S (2)	1770 (1)	−143 (1)	535 (1)	62 (1)
N(1)	446 (1)	1668 (2)	1385 (2)	36 (1)
N(2)	1062 (1)	1313 (2)	1034 (3)	45 (1)
C (1)	1098 (2)	412 (2)	1084 (3)	46 (1)
C(2)	284 (2)	2503 (2)	972 (3)	35 (1)
C(3)	790 (2)	3048 (3)	387 (4)	56 (1)
C(4)	−536 (2)	3922 (2)	1064 (3)	44 (1)
C (5)	−1278 (2)	4065 (3)	1043 (3)	51 (1)
C(6)	−1622 (2)	3184 (3)	990 (3)	46 (1)
C (7)	−1088 (2)	2487 (2)	993 (3)	37 (1)
C (8)	−405 (2)	2939 (2)	1044 (3)	35 (1)
C (9)	−926 (2)	3849 (3)	−2018 (3)	53 (1)
C (10)	−1629 (2)	4192 (3)	−2009 (3)	55 (1)
C (11)	−2096 (2)	3423 (3)	−2046 (3)	60 (1)
C (12)	−1691 (2)	2612 (3)	−2079 (3)	55 (1)
C (13)	−961 (2)	2870 (3)	−2059 (3)	52 (1)
C (14)	2094 (3)	772 (4)	−265 (5)	73 (2)

Equivalent isotropic *U* defined as one third of the trace of the orthogonalized U_{ij} tensor.

2.3.2. PdL_2 **2**

Ethanol solutions (25 ml) of the ligand (0.66 g, 2 mmol), and $PdCl_2(CH_3CN)_2$ (0.26 g, 1 mmol) were mixed. The brown crystalline solid formed after refluxing for 4 h was collected by filtration, washed with ethanol and dried under vacuum. Yield 0.56 g (73%) of the palladium complex. Anal. Found: C, 43.3; H, 3.8; N, 7.1. $C_{28}H_{30}N_4S_4Fe_2Pd$. Calc: C, 43.7; H, 3.9; N, 7.3%. Crystals suitable for X-ray structural analysis were obtained by slow evaporation of a dichloromethane solution in air.

2.3.3. CuL_2 **3**

Ethanol solutions (25 ml) of the ligand (0.66 g, 2 mmol) and $Cu(CH_3COO)_2 \cdot 2H_2O$ (0.20 g, 1 mmol) were mixed. The brown crystalline solid formed after refluxing for 4 h was collected by filtration, washed with ethanol and dried under vacuum. Yield 0.37 g (51%) for the copper complex. Anal. Found: C, 46.2; H, 4.3; N, 8.0. $C_{28}H_{30}N_4S_4Fe_2Cu$ Calc: C, 46.5; H, 4.2; N, 7.7%. Crystals suitable for X-ray structure analysis were obtained by slow evaporation of a dichloromethane solution in air.

2.4. Electrochemistry measurements

Differential-pulse voltammetry was done with an EG and GPAR model 273 instrument, which has a 50 ms pulse width, with current sampled 40 ms after the pulse was applied. A sweep rate of 2 mV s^{-1} was used in all pulse experiments with a drop time of 0.5 s. Cyclic voltammetry was also performed using EG and GPAR model 273 potentiostats in a three-electrodes cell with purged N_2 gas inlet and outlet. The cell comprise of a platinum-wire working electrode, a platinum auxiliary electrode and a Ag/AgCl reference electrode. Current-potential curves were displayed on an IBM computer using model 270 electrochemical analysis software. Data were recorded on a Hewlett–Packard recorder. The voltammograms of the complexes were obtained in dichloromethane with n-Bu_4NClO_4 (0.1 mol dm^{-3}) as the electrolyte and ferrocene (2.0×10^{-3} mol dm^{-3}) as internal standard.

Caution! Although no problems were encountered in this work, the salt perchlorates are potentially explosive. They should be prepared in small quantities and handled with care.

2.5. X-ray data collection and solution

The relevant crystal data and structural parameters are summarized in Table 1. The intensities were collected at 294 K on a Rigaku RAXIS-IIC imaging-plate diffractmeter using Mo–K_α radiation ($\lambda = 0.71073$ Å) from a rotating-anode generator operating at 50 kV and 90 mA ($2\theta_{max} = 55.0°$), 60 oscillation frames in the range of 0–180° are taken, and exposure 8 min per frame for complexes **2** and **3** [5,6].

The two structures were solved by the direct methods. All non-hydrogen atoms were refined anisotropically by full-matrix least-squares. Hydrogen atoms were placed in calculated positions (C–H 0.96 Å), assigned fixed isotropic thermal parameters and allowed to ride on their respective parent atoms. The contributions of these hydrogen atoms were include in the structure-factor calculations. All computations were carried out on a PC-486 computer using the SHELXL-PC program package [7]. Analytical expressions of neutral-atom scattering factors were employed and anomalous dispersion corrections were incorporated [8]. Tables 2 and 3 give atomic coordinates and equivalent isotropic displacement parameters for **2** and **3**, respectively. A complete list of bond lengths and angles and tables of hydrogen atom coordinates as well as anisotropic thermal parameters have been deposited at the Cambridge Crystallographic Data Center (CCDC).

3. Results and discussion

3.1. Synthesis and characterization

The three metal complexes can easily formed by refluxing the mixture of the ligand HL and the metal salt in ethanol. The ν(N–H) in IR spectra (Table 4) of HL exhibits a strong band at 3164 and 3092 cm^{-1}. These bands disappear in the IR spectra of the metal complexes which suggest that the proton on the α-nitrogen atom is lost upon complex formation with a metal ion. A strong band at 1060 cm^{-1} in the IR spectrum of HL is assigned to ν(C=S). After complexation with the metal atoms, this band shifts ca. 60 cm^{-1} to the red region. This observation can be explained by

Table 3
Atomic coordinates (10^4) and equivalent isotropic displacement coefficients ($Å^2 \times 10^3$)

Atom	x	y	z	U_{eq}
Cu (1)	4820 (1)	1646 (1)	4998 (1)	45 (1)
Fe (1)	1887 (1)	1190 (1)	4110 (1)	52 (1)
Fe (2)	5966 (1)	3034 (1)	3094 (1)	53 (1)
S (1)	5886 (1)	886 (1)	5174 (1)	65 (1)
S (2)	6497 (1)	−130 (1)	4187 (1)	74 (1)
S (3)	4559 (1)	1969 (1)	6051 (1)	56 (1)
S (4)	3581 (1)	3174 (1)	6478 (1)	71 (1)
N (1)	4508 (2)	1089 (1)	4194 (1)	45 (1)
N (2)	5120 (2)	611 (1)	3972 (2)	53 (1)
N (3)	4475 (2)	2613 (1)	4730 (1)	47 (1)
N (4)	4033 (2)	2995 (2)	5220 (2)	53 (1)
C (1)	5738 (2)	498 (2)	4400 (2)	53 (1)
C (2)	3850 (2)	1151 (2)	3790 (2)	44 (1)
C (3)	3821 (2)	799 (2)	3120 (2)	63 (1)
C (4)	3117 (2)	1567 (1)	4002 (2)	43 (1)
C (5)	2817 (2)	1666 (2)	4672 (2)	53 (1)
C (6)	2058 (2)	2078 (2)	4648 (2)	69 (1)
C (7)	1885 (2)	2235 (2)	3979 (2)	73 (1)
C (8)	2521 (2)	1922 (2)	3560 (2)	57 (1)
C (9)	1463 (2)	424 (2)	3504 (2)	119 (1)
C (10)	1930 (2)	145 (2)	4061 (2)	93 (1)
C (11)	1504 (2)	337 (2)	4628 (2)	90 (1)
C (12)	785 (2)	728 (2)	4459 (2)	98 (1)
C (13)	746 (2)	780 (2)	3771 (2)	103 (1)
C (14)	6191 (2)	−332 (2)	3345 (2)	99 (1)
C (15)	4060 (2)	2732 (2)	5810 (2)	49 (1)
C (16)	4465 (2)	2885 (2)	4141 (2)	49 (1)
C (17)	3944 (2)	3511 (2)	3985 (2)	71 (1)
C (18)	4795 (2)	2593 (2)	2909 (2)	57 (1)
C (19)	5772 (2)	2187 (2)	3684 (2)	50 (1)
C (20)	6059 (2)	1983 (2)	3042 (2)	58 (1)
C (21)	5451 (2)	2231 (2)	2562 (2)	59 (1)
C (22)	4979 (2)	2574 (2)	3614 (2)	47 (1)
C (23)	7013 (2)	3552 (2)	3433 (2)	105 (1)
C (24)	6274 (2)	3957 (2)	3506 (2)	130 (1)
C (25)	5925 (2)	4055 (2)	2867 (2)	117 (1)
C (26)	6449 (2)	3724 (2)	2435 (2)	115 (1)
C (27)	7118 (2)	3418 (2)	2782 (2)	109 (1)
C (28)	3145 (2)	3914 (2)	6071 (2)	99 (1)

Equivalent isotropic U defined as one third of the trace of the orthogonalized U_{ij} tensor.

Table 4
Spectroscopic and electrochemistry data of the ligand and the metal complexes

	IR spectra (cm^{-1})		UV–vis λ (nm) (logε)		Cyclic voltammogram[a] vs. AgCl/Ag (V)				Different pulse voltammogram (V)	
HL	ν(N–H)	3092, 3164	L–L*	200 (4.33)	Epc	0.65	0.77		$E_{1/2}$	0.62
	ν(C=N)	1595, 1500		240 (4.46)	Epa	0.59	0.71			0.74
	ν(C=C)	1457, 1420		322 (4.42)	$E_{1/2}$	0.62	0.74			
	ν(C–S)	958, 1060	MLCT	465 (3.51)						
	δ(C–H)	816								
1	ν(C=N)	1556	L–L*	200 (4.68)	Epc	0.65	0.88	1.02	$E_{1/2}$	0.62
	ν(C=C)	1460, 1425		240 (4.78)	Epa	0.59	0.82	0.96		0.85
	ν(C–S)	1005, 946		273 (4.60)	$E_{1/2}$	0.62	0.85	0.98		0.98
	δ(C–H)	822		344 (4.09)	ΔE	0.13			ΔE	0.13
	ν(Ni–N) 386	386	MLCT	468 (3.81)						
	ν(Ni–S) 328	328	d–d	660 (solid)						
2	ν(C=N)	1563	L–L*	200 (4.70)	Epc	0.65	0.83	0.98	$E_{1/2}$	0.62
	ν(C=C)	1462, 1425		240 (4.75)	Epa	0.59	0.77	0.93		0.78
	ν(C–S)	1006, 941		273 (4.55)	$E_{1/2}$	0.62	0.80	0.95		0.96
	δ(C–H)	823		344 (4.26)	ΔE	0.15			ΔE	0.18
	ν(Pd–N)	372	MLCT	476 (3.76)						
	ν(Pd–S)	325	d–d	590 (solid)						
3	ν(C=N)	1562	L–L*	200 (4.66)	Epc	0.65	0.85		$E_{1/2}$	0.62
	ν(C=C)	1465, 1427		240 (4.76)	Epa	0.59	0.75			0.81
	ν(C–S)	1005, 943		273 (4.50)	$E_{1/2}$	0.62	0.80			
	δ(C–H)	823		348 (4.13)						
	ν(Cu–N)	361	MLCT	477 (3.87)						
	ν(Cu–S)	330	d–d	784 (solid)						

[a] Cyclic voltammogram in the anodic region at scanning ratre of 50 mV s^{-1} in CH_2Cl_2 solution containing n-Bu_4NClO_4 (0.1 M) as electrolyte. The first half-wave potential is the internal standard ferrocenium/ferrocene.

the change in the nature of the C=S bond on coordination of the ligand through the sulfur atom. It suggests that the deprotonation may be attributed to the stabilization by conjugation of the –C=N–N=C– group [12]. This suggestion was supported by crystal structure determination of the relative ligands and their metal complexes [4,9–11]. The far-IR spectra (500–l00 cm^{-1}) of the complexes display a medium to strong band in the region 385–345 cm^{-1} which can be assigned to the metal–nitrogen stretching vibrations [13,14], and in most case, another band in the range 336–356 cm^{-1}, may be assigned to the metal–sulfur stretching frequencies [15].

The visible spectra are consistent with the structural formulates (Table 1), the broad band at ca. 450–470 nm is assigned to the MLCT band of ferrocene and the bridging metal moiety which coupled each other [9–11]. Three bands corresponding to the transition $^1A_{1g} \leftarrow {}^1A_{2g}$, $^1A_{1g} \leftarrow {}^1B_{1g}$ and $^1A_{1g} \leftarrow {}^1E_g$ are expected in the electronic spectrum of a square-planar d_8 complex. However, in many instances, especially with sulfur ligands, the bands corresponding to the transitions $^1A_{1g} \leftarrow A_{2g}$, $^1A_{1g} \leftarrow {}^1B_{1g}$ and $^1A_{1g} \leftarrow {}^1E_g$ are submerged under very intense inter-ligand and charge transfer band, and only one band in the range 620–500 nm is observed. The shoulder is around 660 nm for the nickel complex, 590 nm for the palladium complex in the solid electronic reflectance therefor may be assigned to the $^1A_{1g} \leftarrow {}^1A_{2g}$ transition [16]. The electronic spectrum of the Cu(II) chelate in Nujol mull shows only one broad band with a maximum at 784 nm. The appearance of only one band at 780 nm might indicate that the coordination geometry of the copper is a distorted configuration between square-planar and tetrahedral [14].

3.2. Structure of palladium complex PdL_2 **2**

Fig. 1 shows an ORTEP drawing of the molecule with the atomic numbering scheme. The Pd(II) atom is coordinated in slight distorted square-planar configuration with 2 equiv. Pd–N bonds (2.110(3) Å) and Pd–S bonds (2.257(1) Å). The dihedral angle between the two coordination planes is 4.0°. The ligand, as expected, losses a proton from the tautomeric thiol form and acts as a single negatively charged bidentate ligand coordinating to the palladium ion via the mercapto sulphur and β-nitrogen atoms [9–11], forming delocalized plane. The complex has a quite surprising *cis*-configuration (N(1)–Pd(1)–N(1A), 106.1(1)°, S(1)–Pd(1)–S(1A), 89.0(1)°, symmetry code: A: $-x$, y, $0.5-z$) with two ferrocene moieties on the same side. The structure is

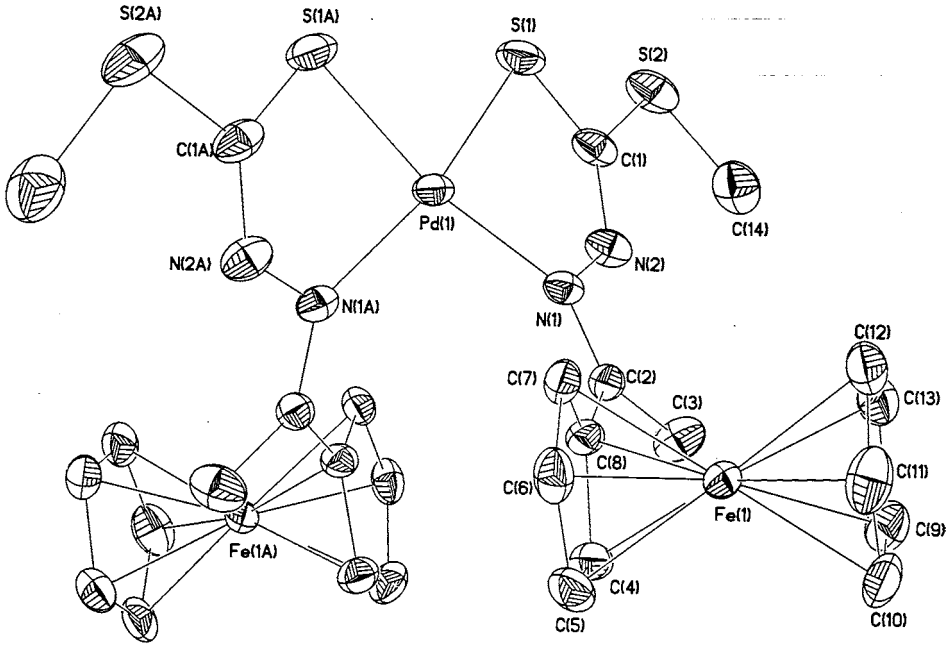

Fig. 1. ORTEP drawing of the molecule of PdL_2 complex **2**, showing also the labeling of the atoms. Thermal ellipsoids are drawn at 30% probability level. Symmetry codes: *a*, $-x$, y, $0.5-z$.

much rare, to our knowledge, this might be the first example for the negatively charged bidentate thiocarbazates coordinate in *cis*-configuration [17,18]. It suggests that the *cis*-configuration was stabilized by the interactions between the two substituted cyclopentadienyl planes associated with difference iron atoms. Least-square planarity analyses shows that the two acetytylcyclopentadienyl ring are almost parallel each other (dihedral angle of 2.9°). The methylene carbon atoms C(2) is less than 3.0 Å from the substituted cyclopendatienyl plane formed by C(4A), C(5A) C(6A), C(7A) and C(8A), and the shortest interatomic distances, C(2)···C(7A) is ca. 3.3 Å.

Considering the van der Waals radius for a methylene group and the half-thickness of an aromatic ring [19], the pull contacts might be strong and apparently determine the *cis*-positioning of the two ferrocene moieties. The bond distances (Table 5) in the side chain are intermediate between formal single and double bonds, pointing to electron delocalization over the entire moiety. The Pd···Fe distance is ca. 5.10 Å and the Fe···Fe distance is 7.02 Å. Those separation are much larger than those found in most biferrocene compounds (3.8–5.1 Å) and much closer to the average encounter distance between ferrocene and ferrocenium ion in solution (7.6 Å) [20].

Table 5
Selected bond lengths (Å) and angles (°)

	Bond lengths		Angles	
2	Pd(1)–S(1)	2.257(1)	S(1)–Pd(1)–N(1)	82.8(1)
	Pd(1)–N(1)	2.110(3)	S(1)–Pd(1)–S(1a)	89.0(1)
	S(1)–C(1)	1.738(4)	N(1)–Pd(1)–S(1a)	169.3(1)
	S(2)–C(1)	1.747(4)	N(1)–Pd(1)–N(1a)	106.1(1)
	N(1)–N(2)	1.420(4)		
	N(1)–C(2)	1.295(4)		
	N(2)–C(1)	1.300(4)		
3	Cu(1)–S(1)	2.239(1)	S(1)–Cu(1)–S(3)	99.9(1)
	Cu(1)–S(3)	2.228(1)	S(1)–Cu(1)–N(1)	86.8(1)
	Cu(1)–N(1)	1.994(3)	S(3)–Cu(1)–N(1)	150.1(1)
	Cu(1)–N(3)	2.029(3)	s(1)–Cu(1)–N(3)	148.0(1)
	S(1)–C(1)	1.733(4)	S(3)–Cu(1)–N(3)	86.5(1)
	S(3)–C(15)	1.741(3)	N(1)–Cu(1)–N(3)	103.3(1)
	N(1)–N(2)	1.398(4)		
	N(1)–C(2)	1.301(4)		
	N(2)–C(1)	1.298(4)		
	N(3)–N(4)	1.403(4)		
	N(3)–C(16)	1.289(4)		
	N(4)–C(l5)	1.284(4)		

Symmetry code *a*: $-x$, y $0.5-z$.

3.3. Crystal structure of the copper complex CuL_2

Fig. 2 shows an ORTEP drawing of the molecule with the atomic numbering scheme. The Cu(II) atom is coordinated in distorted tetrahedral configuration with two Cu–N bonds (2.029(3), 1.994(3) Å) and Cu–S bonds (2.239(1), 2.228(1) Å). The dihedral angle between the two coordination planes is 42.9°. The ligand, as expected, also losses a proton from the tautomeric thiol form and acts as a single negatively charge bidentate ligand coordinating to the copper ion via the mercapto sulphur and (-nitrogen atoms, forming an electron delocalized coordination plane. The two copper–iron distances are almost equivalent (Cu–Fe ca. 4.96 Å). The distance between the iron–iron is 7.51 Å.

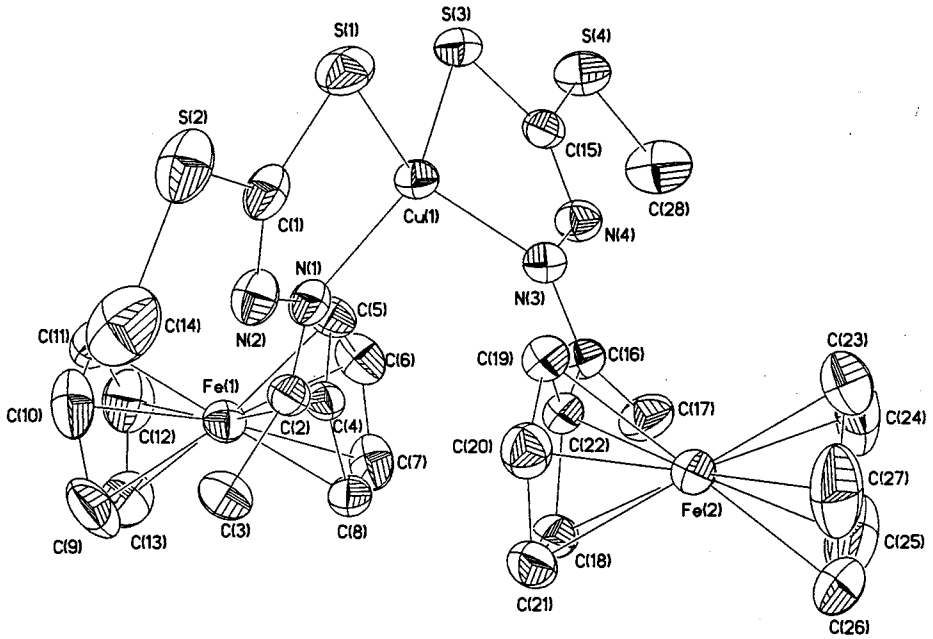

Fig. 2. ORTEP drawing of the molecule of CuL_2 complex **3**, showing also the labeling of the atoms. Thermal ellipsoids are drawn at 30% probability level.

3.4. Electrochemistry studies

The half-wave potentials ($E_{1/2}$) (Table 4) of the redox processes and the separation between consecutive waves (ΔE) vary depending on the nature of the complexes and their geometric structures. The internal standard, ferrocene, undergoes a reversible one-electron oxidation as expected ($E\text{pa} = 0.59$, $E\text{pc} = 0.65$ V vs. Ag/AgCl electrode, scanning rate 50 mV s^{-1}), The ligand HL (2.0×10^{-3} mol dm^{-3}) undergoes a reversible one-electron oxidation($E\text{pa} = 0.77$ V, $E\text{pc} = 0.71$ V vs. Ag/AgCl electrode, scanning rates, 50 mV s^{-1}). The metal-bridged biferrocene complexes **1** and **2** like many homobinuclear species, show two sequential reversible one-electron oxidation E_1 and E_2, separated by ΔE (Fig. 3a) to yield the mono- and dications, respectively.

$$[\text{Fc–M–Fc}]\ [\text{Fc–M–Fc}]\ [\text{Fc–M–Fc}] \quad (1)$$

$$[\text{Fc–M–Fc}] + [\text{FcMFc}]\ 2[\text{Fc–M–Fc}] \quad (2)$$

Where Fc represents a ferrocenyl unit and M represents the metal moiety of bridging group. The equilibrium constants K_{com} of the equation can be calculated by use of the Nernst equation from the ΔE (Table 4). It is interesting to note that complex **3** exhibits a single voltammetric wave (Fig. 3b) and the half-wave potential $E_{1/2}$ does not vary with scanning rate, however, the large peak-to-peak separation ($\Delta E\text{p} = E\text{pa} - E\text{pc}$) of 100 mV (scanning rate of 50 mV s^{-1}) might suggest that this peak was not a simple reversible one-electron reaction. It has been postulated that a statistical contribution of 36 mV ($K_{\text{com}} = 4$) holds for identical, noninteracting metal ions in the homobinuclear complexes, the small ΔE value (36 MV) between two voltammetric waved always led to the two waves coupled each other and only one broad voltammetric wave appeared in the cyclic voltammetry measurements. In this case, the only one broad voltammetric wave in the Cu(II) bridged biferrocene complex **3** indicates that the two ferrocene moieties are identical and there is no interaction between them.

As in the cyclic case, a simple sum of two n-electron responses can not be used to determine ΔE, except when the value is larger. It has been postulated that, when $\Delta E > 160$ mV, an error of < 1 mV will be introduced, if the peak separation is used to measure the value. In order to measure the ΔE more precise, we use the pulse voltammetry to repeat the electrochemistry measurement (Fig. 4). The peak at ca. 0.62 V is simply assigned to redox reaction of ferrocene, the internal standard. In Fig. 4c, another peak is assigned to the redox reaction of complex **3**, it has also been suggested that the broadening of this peak might contribute to two oxidation reaction coupled each other. Fig. 4a and b show the different pulse curve of complexes **1** and **2**, respectively, the ΔE value can be easily obtained as 0.13 and 0.18 V for the complexes **1** and **2**, respectively.

It is postulated that the ΔE with K_{com} depends on a number of factors [21–27] (1) Major structural changes such as bond making and breaking, changes in coordination number, and severe changes in coordination geometry upon charge transfer can shift comproportionation equilibrium. (2) If the metal ions are in close proximity, a through-space coulomb interaction may be

important. A n^+ ion will be more readily reduced than a $(n^+)^-$ ion on basis of electrostatic consideration alone. This will increase ΔE and hence K_{com}. (III) Electronic delocalization in mixed oxidation states will enhance the stability of these species with resulting increases in ΔE.

The trinuclear complexes, **1** and **2** together with the Cu(II) complex **3**, were designed to help quantitatively define some of these effects. (1) Although the bridged metal moieties can accommodate a range of coordination geometry, it is likely that only negligible structural changes accompany one-electron oxidation of the complexes, since crystallographic data on ferrocene [28] and its salts [29] indicate that the oxidation state and charge of the iron atom have almost no effect on the interatomic distances. (2) Through space metal–metal coulomb contribution to the Fe(II)/Fe(III) oxidation potential in Fc–M–Fc complexes are essentially constant and could be cancelable, since the distances between iron atoms are almost same for the two metal bridged biferrocene complexes **2** and **3**, and are quite

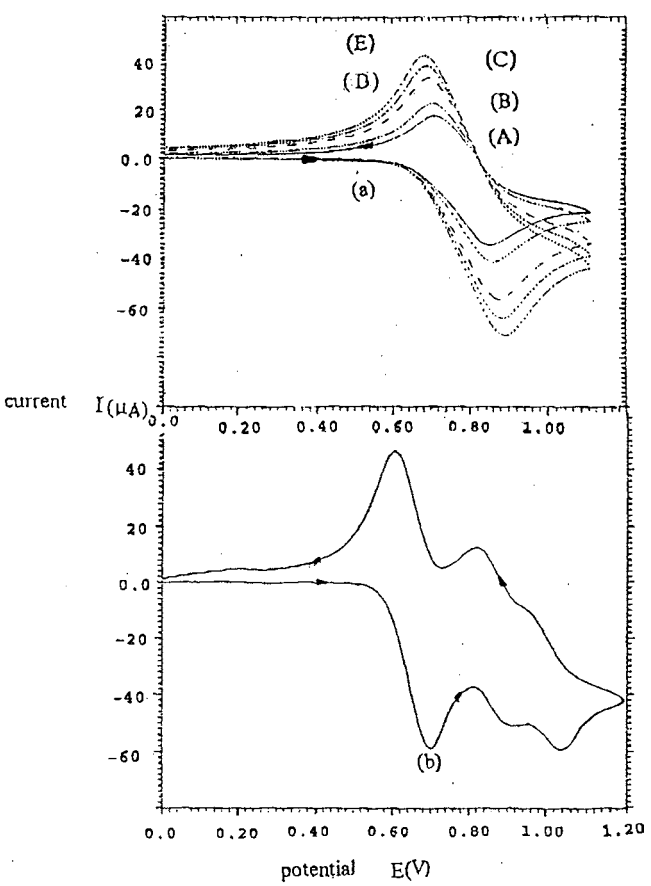

Fig. 3. Cyclic voltammogram of the complexes in CH_2Cl_2 containing n-Bu_4NClO_4 (0.1 M); (a) NiL_2 (1.0×10^{-3} M) at scanning rate of 50 mV s^{-1} with ferrocene (2.0×10^{-3} M) as internal standard. (vs. AgCl/Ag); (b) CuL_2 (1.0×10^{-3} M) at different scanning rates (vs. AgCl/Ag); (A) 50 mV s^{-1}; (B) 75 mV s^{-1}; (C) 150 mV s^{-1}; (D) 200 mV s^{-1}; (E) 250 mV s^{-1}.

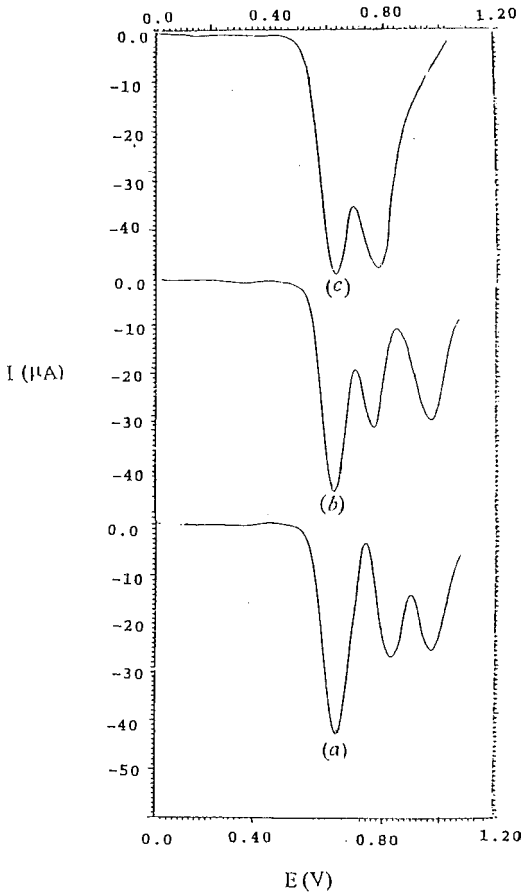

Fig. 4. Current-Cornell University, Press, Itha-pulse voltammetry for the three complexes (1.0×10^{-3} M) in CH_2Cl_2 containing n-Bu_4NClO_4 (0.1 M) and internal standard (ferrocene 2.0×10^{-3} M) (vs. AgCI/Ag (a) NiL_2, (b) PdL_2, N.Y., (1) CuL_2.

close to 7.6 Å, the average encounter diameter between ferrocene and ferricenium ion in solution. In fact, these metal-bridged biferrocen complexes designed here are used to minimize the through space iron-iron interaction between the ferrocene moieties. (3) The electrochemistry for these metal bridges complexes accounts for structural, Coulomb as explained above. The difference in electrochemistry of complexes **2** and **3** then can be described to the difference in stability associated with a degree of electronic delocatopn in the complexes. Crystal structure analysis indicates that the metal–iron and iron–iron distances as well as the bond distances of the ferrocene moieties are almost equivalent for these complex **2** and **3**, the only difference of the two molecular structures in the coordination geometry of the bridged metal moieties. This result demonstrated that the different in electrochemistry of complexes **2** and **3** should be contributed to the difference of the coordination geometry of the bridged metal moieties. In complex **2**, the center metal palladium coordinated in square-planar configuration, the empty d_z2 orbital can allow the electron moving in the whole molecule freely, while in complex **3**, the tetrahedral coordinated cop-

per(II) can not stabilized can minimize the electron transfer in the whole molecule. In light of the electrochemical data and structural data, some prediction are clearly not borne out. First, the metal-iron and iron–iron distance are not the important factors influence the redox potentials of these kind of metal bridged biferrocene complexes.

Acknowledgements

This work was supported by the National Nature Science Foundation of China.

References

[1] D.N. Hendrickson, S.M. Oh, T.Y. Dong, T. Kambara, M.J. Cohn, M.F. Moore, Comment. Inorg. Chem. 4 (1985) 329.
[2] R.J. Webb, T.Y. Dong, C.G. Pierpont, S.R. Boone, R.K. Chadha, D.N. Hendrickson, J. Am. Chem. Soc. 113 (1991) 4806.
[3] P. Shu, K. Bechgaard, D.O. Cowan, J. Org. Chem. 41 (1976) 1849.
[4] C.Y. Duan, X.B. Xia, L.G. Zhu, X.Z. You, Y. Yang, H.Q. Wang, Chinese J. Chem. 12 (1994) 321.
[5] J. Tanner, K. Krause, Riguka J. 11 (1994) 4; ibid. 7 (1990) 28.
[6] K.L. Kraus, G.N. Phillips, J. Appl. Crystallogr. 25 (1992) 146.
[7] G.M. Sheldrick, in: D. Sayre (Ed.), Computional Crystallography, Oxford University Press, New York, 1982, pp. 506–514.
[8] International Tables for X-ray Crystallography, vol. 4, Kynoch Press, Birmingham (now distributed by Kluwer Academic Press, Dordrecht), 1974, pp. 55, 99, 149.
[9] Y.P. Tian, C.Y. Duan, Z.L. Lu, X.Z. You, J. Coord. Chem. 38 (1996) 219.
[10] Y.P. Tian, C.Y. Duan, Z.L. Lu, X.Z. You, Polyhedron 15 (1996) 2263.
[11] Y.P. Tian, C.Y. Duan, Z.L. Lu, X.Z. You, Transit. Met. Chem. 21 (1996) 254.
[12] B.A. Gingras, A.F. Sirianni, Can. J. Chem. 42 (1964) 17.
[13] D.M. Adams, Metal–Ligand and Related Vibrations, Arnold, London, 1967.
[14] D.M. Adams, J.B. Correll, J. Chem. Soc. A (1968) 1299.
[15] (a) M.T.H. Tarafder, M.A. Ali, Can. J. Chem. 56 (1978) 2000. (b) S.E. Livingstone, J.D. Nolan, Aust. J. Chem. 26 (1973) 961.
[16] A.R. Lathan, V.C. Hascall, H.B. Gray, Inorg Chem. 4 (1965) 783.
[17] S. Podhye, G.B. Kauffman, Coord Chem. Rev. 63 (1985) 127.
[18] (a) M.A. Ali, S.E. Livingstone, Coord. Chem. Rev. 13 (1974) 101. (b) M. J. M.Campbell, Coord. Chem. Rev. 15 (1975) 279.
[19] L. Pauling, The Nature of the Chemical Bond, 3rd ed., Cornell University Press, Ithaca, N.Y., 1960, p. 260.
[20] D.R. Stank, Discuss. Faraday Soc. 29 (1960) 73.
[21] M.B. Robin, P. Day, Adv. Inorg. Chem. Radiochem. 10 (1967) 247.
[22] C. Creutz, H. Taube, J. Am. Chem. Soc. 95 (1973) 1086.
[23] R.W. Callahan, F.R. Keene, T.J. Mayer, D.J. Salmon, J. Am. Chem. Soc. 96 (1974) 7827.
[24] G.M. Tom, C. Creutz, H. Taube, J. Am. Chem. Soc. 96 (1974) 7828.
[25] T.R. Weaver, T.J. Mayer, S.A. Adeylmi, G.M. Brown, R.P. Eckberg, E. Hatfield, E.C. Johnson, R.W. Murray, D. Unterker, J. Am. Chem. Soc. 97 (1975) 3039.
[26] W.H. Morrison Jr., S. Krogsrud, D.N. Hendrickson, Inorg. Chem. 12 (1973) 1998.
[27] R.R. Gagne, C.L. Spiro, T.I.. Smith, C.A. Hamann, W.R. Thies, A.K. Shiemke, J. Am. Chem. Soc. 103 (1981) 4073.
[28] Rosenblum, Chemistry of the Iron Group Metallocenes, New York, 1965.
[29] T. Berstern, F.H. Herbstein, Acta Crystallogri Sect B 24 (1968) 1546.